

National Snow and Ice Data Center
Cooperative Institute for Research in Environmental Sciences

Validation Studies and Sensitivity Analyses for Retrievals of Snow Albedo from EOS AM-1 Instruments

Progress Report for Year 2000-2001

**Anne W. Nolin
Principal Investigator**

**Julienne C. Stroeve
Co-Investigator**

University of Colorado - Boulder
Home Page: <http://www-nsidc.colorado.edu/PROJECTS/ALBEDO>

August 22, 2001

Table of Contents

<u>1.</u>	<u>BACKGROUND AND COMPLETED WORK</u>	1
<u>1.1</u>	<u>PROJECT SUMMARY</u>	1
<u>1.2</u>	<u>LIST OF OBJECTIVES</u>	1
<u>1.3</u>	<u>PREVIOUS WORK COMPLETED</u>	1
<u>2.</u>	<u>PROGRESS IN YEAR 2000-2001</u>	1
<u>2.1</u>	<u>COLORADO FIELD EXPERIMENT</u>	2
<u>2.2</u>	<u>NARROWBAND-TO-BROADBAND ALBEDO CONVERSION MODELING</u>	5
<u>2.3</u>	<u>COMPARISON OF MODIS AND MISR ALBEDOS WITH IN SITU DATA</u>	7
<u>3.</u>	<u>COLLABORATIONS</u>	10
<u>4.</u>	<u>PLANNED WORK FOR 2001-2002</u>	10
	<u>RELEVANT PUBLICATIONS FOR 2000-2001</u>	11

1. Background and Completed Work

1.1 *Project Summary*

As part of NASA's effort to map and characterize the Earth system from space, this investigation is engaged in validating snow albedo retrievals from instruments on board Terra, the Earth Observing System satellite. Surface albedo, the surface hemispheric reflectivity integrated over the solar spectrum, is a fundamental component needed for determining the radiation balance of the Earth-atmosphere system. Because snow is strongly forward scattering and has a variable albedo across the solar spectrum, spaceborne measurements in a few channels and one or few viewing angles are not representative of the spectrally integrated albedo. In addition to validation activities we are also undertaking sensitivity studies to investigate how atmospheric properties, topographic complexity and spatial resolution affect albedo retrievals.

Surface albedo will be one of the standard data products to be generated from data acquired by the Moderate Resolution Imaging Spectroradiometer (MODIS) instrument. The Multiangle Imaging SpectroRadiometer (MISR) requires characterization of the angular reflectance characteristics over snow. A critical concern is the current lack of an aerosol retrieval method that provides accurate estimates over snow-covered surfaces. This prevents accurate atmospheric correction of MODIS and MISR data over snow. Through a combination of model simulations and field validation experiments (both pre-launch and post-launch) this research is validating a scheme for converting measurements of snow bidirectional reflectance to snow albedo for both MODIS and MISR. A narrowband-to-broadband conversion is being developed and tested for both instruments allowing intercomparison of broadband albedo retrievals between MODIS and MISR. In sensitivity analyses, we are evaluating how atmospheric characterizations affect the accuracy of narrowband albedo retrievals and derived broadband albedo estimates.

1.2 *List of Objectives*

1. Evaluate snow albedo retrievals from MODIS and MISR
 - Validate snow BRDF model
 - Quantify sensitivity of snow albedo estimates to atmospheric variables
2. Develop and test a narrowband-to-broadband snow albedo conversion scheme for MODIS and MISR
3. Perform intercomparisons of broadband snow albedo estimates from MODIS and MISR

1.3 *Previous work completed*

- Developed and tested a hemispherical directional reflectance factor (HDRF)-to-albedo conversion scheme for MODIS and MISR
- Modeled MODIS and MISR albedo sensitivities to atmospheric variables
- Field data collection in California (pre-launch) and Greenland (post-launch)
- Developed narrowband-to-broadband coefficients for MODIS and MISR
- Examined sensitivity of MISR albedo estimates to DEM accuracy

2. Progress in Year 2000-2001

Efforts in this past project year have focused on three tasks:

1. Acquiring and analyzing ground-based and airborne data from our February-March field experiment in Steamboat Springs, Colorado
2. Comparing MODIS- and MISR-derived HDRF, narrowband and broadband albedo values over validation sites in Greenland
3. Modeling sensitivities of the narrowband-to-broadband conversion models to atmospheric parameters and snow grain size

Results from each of these tasks are presented in the following sections.

2.1 Colorado Field Experiment

Over a five-week period from February 3 to March 8, 2001, we held a field experiment in the Yampa Valley, just south of Steamboat Springs, Colorado. The valley is broad and relatively flat, and typically experiences heavy snowfall during the winter months. The experiment site was the Mills Ranch (40.4° N, 106.8° W, elevation 2100m) on the east side of the valley, where the local landowner provided access to a barn and extensive snow-covered fields. Figure 1 is an AirMISR image that shows the valley and the experiment site. On March 8, 2001, an ER-2 flight successfully acquired AirMISR and MAS data concurrent with numerous ground-based instruments. Additional ground-based measurements were acquired over the period February 3 – March 4, 2001. Ground-based instrumentation included Kipp & Zonen albedometer, ASD Fieldspec FR spectroradiometer with cosine collector, PARABOLA (sphere-scanning radiometer), MFRSR, Cimel and Reagan sun photometers and snow density and grain size measurement tools.

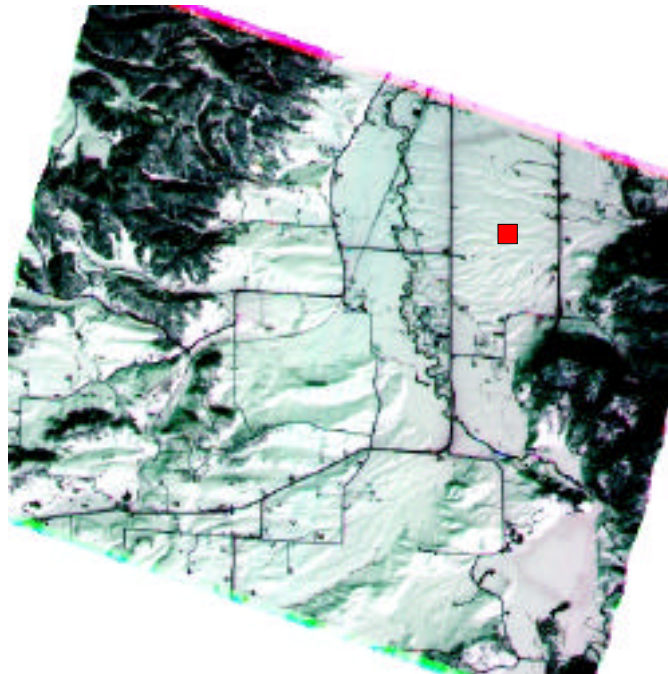


Figure 1. AirMISR color composite of the southern portion of the Yampa Valley. The experiment site is marked by the red square.

The objectives of the experiment were to

- characterize atmospheric conditions for determining surface HDRF values from MISR, MODIS, AirMISR and MAS imagery
- characterize the snow physical properties (grain size, density, stratigraphy)
- compare HDRF values from MISR, MODIS, MAS, AirMISR, and PARABOLA
- further validate snow BRDF model using PARABOLA data
- test the MODIS, MISR, MAS, and AirMISR narrowband-to-broadband albedo conversion models

Instrumentation and technical support for the experiment were generously provided by the MISR project. Overall, the project was a success with nearly all the required data collected in order to meet these objectives. However, because of cloudy conditions on all MISR overpass days throughout the 5-week period, MISR data were not collected concurrent with any of the ground-based measurements. While not all of the data have been analyzed, our results to date have borne out the overall methodology of the HDRF-to-albedo scheme and indicate significant progress. Particularly useful are the data collected by PARABOLA, the sphere-scanning spectroradiometer. We followed the PARABOLA data collection, calibration and analysis scheme as described in Abdou, et al. (JGR, vol. 106, pp. 11967-11976, 2000). For atmospheric correction of all imagery, we used a modified version of the 6S atmospheric correction code (snow substrate was added) to convert from bi-directional reflectance factor (BRF) at the aircraft altitude to surface HDRF. Conversion factors to convert surface HDRF to surface albedo were computed using the DISORT model and measured atmospheric conditions. The conversion factors take the form of DISORT-computed albedo divided by DISORT-computed HDRF, where the HDRF value depends on solar zenith, viewing zenith, and relative sun-sensor azimuth. Measured values of spectral HDRF are then multiplied by the conversion factor that corresponds to the solar and viewing geometry, to obtain spectral albedo.

Results obtained from PARABOLA at the time of the ER-2 overpass (1800 GMT) are shown in figure 2. This figure shows the angular variation of HDRF in the principal plane (solar zenith=48.8°, solar azimuth=155°) for the blue and near-infrared channels of PARABOLA. Data from the red channel are excessively noisy while data from the green channel closely resemble those in the blue channel. In agreement with model results (not shown) the HDRF values peak in the forward-scattering direction. The “bump” in HDRF values at 0-10 degrees is the reflectance of the Spectralon reference panel. Superimposed on the plot are the surface HDRF values obtained from the atmospherically-corrected AirMISR image. Only the central five of the nine AirMISR cameras effectively imaged the site. Thus, only the viewing angles 47.6°, 28.8°, 7.9°, -25.9°, -44.9° are shown. Because of high winds aloft, the ER-2 was not able to fly absolutely level; hence the angles are slightly different from those of the MISR instrument. The AirMISR and PARABOLA HDRF data show excellent agreement. This is the first such comparison of multiangular airborne and ground-based data over snow.

Figure 3 shows the relationship between measured snow albedo from the ASD FieldSpec FR (with cosine receptor) and AirMISR albedo computed using the DISORT-derived conversion factors. AirMISR albedo values in the visible channels show excellent agreement with the ASD albedo values. It is not clear why the ASD near-infrared value is lower than the AirMISR value. We will examine calibration issues for the ASD instrument and AirMISR, as well as error in the NIR conversion factor.

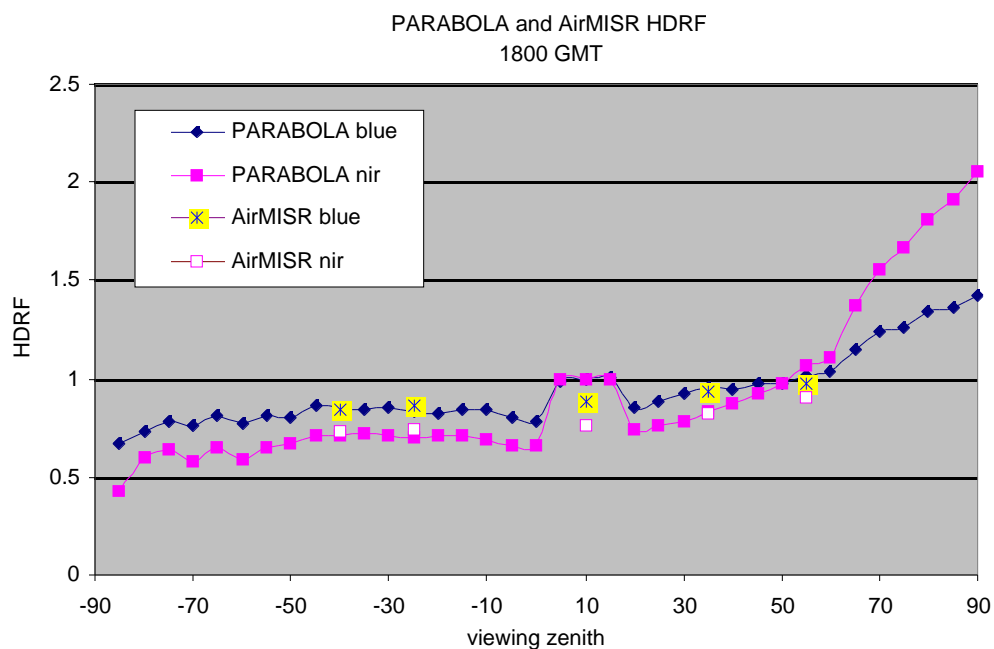


Figure 2. Hemispherical-directional reflectance factor (HDRF) values measured by PARABOLA and AirMISR. In the near-infrared channel, snow is more forward scattering than in the blue channel causing the higher peak reflectance at oblique viewing angles. The “bump” in the middle is the reflectance off of the Spectralon reference panel.

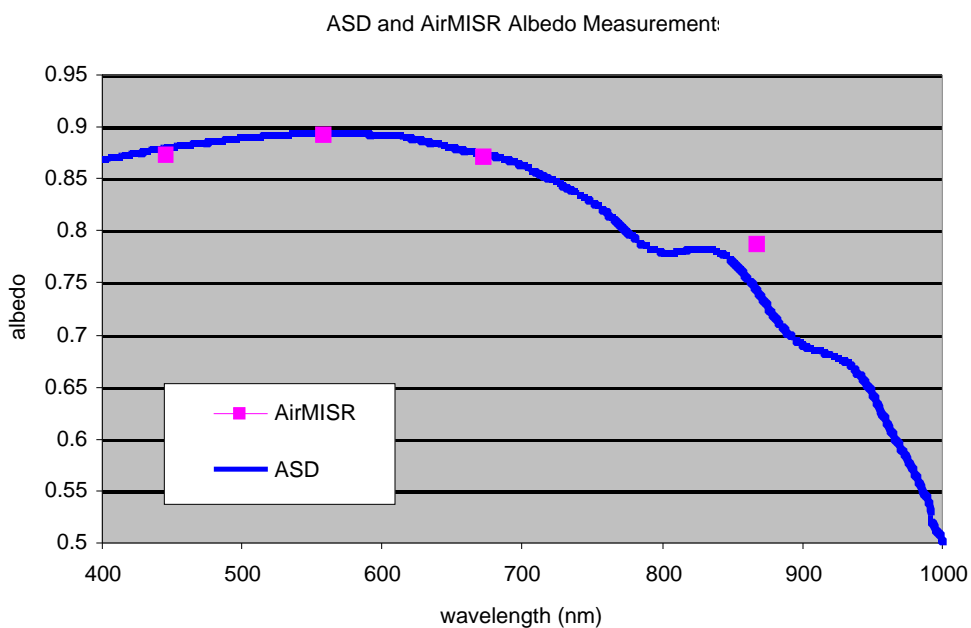


Figure 3. Spectral albedo values for the snowpack surface from ground-based measurements (ASD) and the AirMISR instrument on the ER-2 at 20km

2.2 Narrowband-to-Broadband Albedo Conversion Modeling

To derive broadband surface albedo from narrowband satellite observations, such as from MISR, MODIS or AVHRR requires some sort of conversion. The assumption of a linear relationship is found to be valid for ground-based measurements of narrowband and broadband albedo. For example, figure 4 shows a scatter plot of MISR narrowband albedo versus broadband albedo derived from spectral and broadband albedo measurements collected at a site on the Greenland ice sheet during 1990, 1991 and 1993. Using all four MISR channels as a predictor for the broadband albedo, a relationship such as that in figure 5 develops. Note however, that although the data represent a variety of snow types, ranging from fine-grained new snow to coarse-grained melting snow, the measurements do not represent a wide range of atmospheric and solar zenith angle conditions.

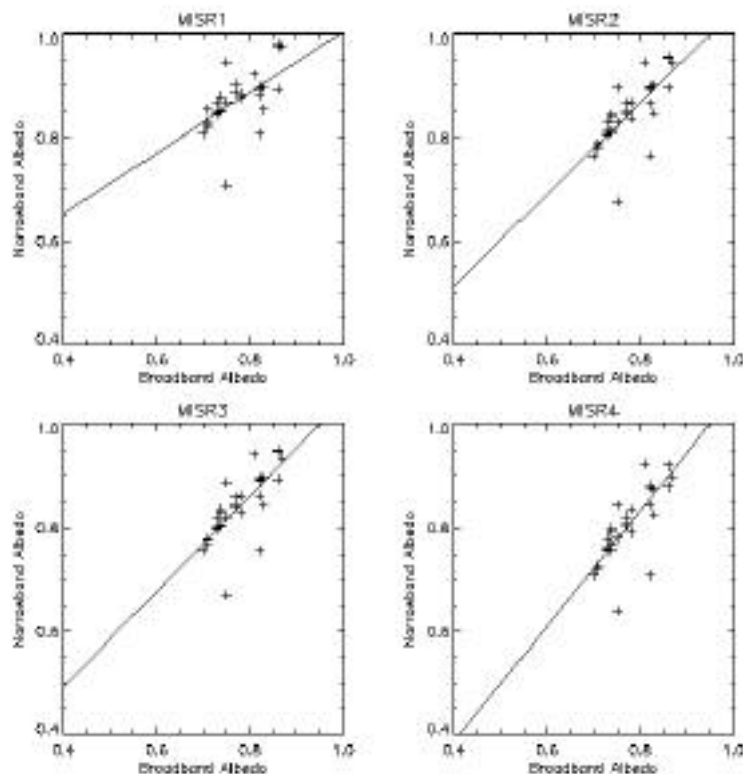


Figure 4. Narrowband vs. broadband plots for each MISR channel. The line represents the best fit.

The conversion from narrowband to broadband albedo not only depends on surface conditions, it also depends on atmospheric conditions. The spectral distribution solar irradiance at the surface is the weighting function for converting the narrowband albedos to broadband albedos. Thus, a relationship developed under a specific surface/atmospheric condition may not be valid under different conditions from which the relationship was developed. This is one reason why published narrow-to-broadband relationships differ widely.

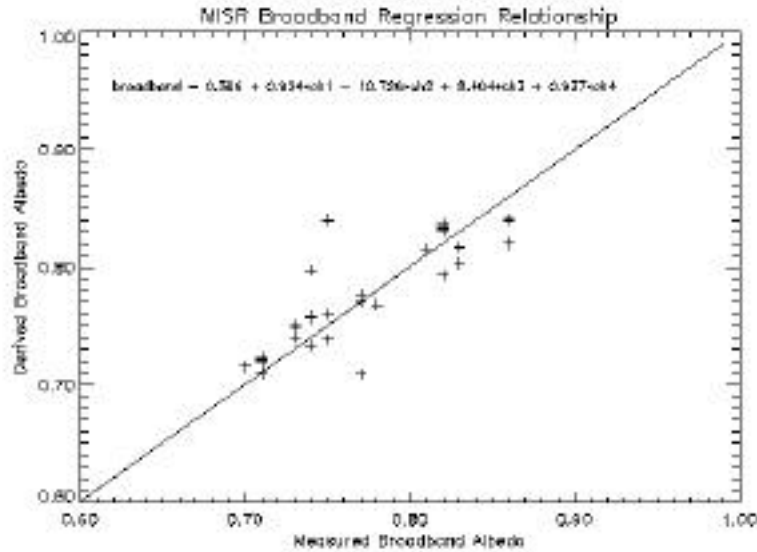


Figure 5. Derived vs. measured broadband albedo using the MISR narrowband-to-broadband regression model.

One means of developing a more general conversion model is to use modeled spectral and broadband albedo under a variety of surface and atmospheric conditions. Using the 6s radiative transfer model, the direct and diffuse solar irradiance components as a function of atmospheric model (arctic summer and arctic winter atmospheric profiles), aerosol optical depth (0.01, 0.05 and 0.10), aerosol model (continental, maritime, desert and urban) and solar zenith angle (0-85° in steps of 5°) are obtained. This information can then be used as input to the DISORT model to obtain the spectral and broadband albedo for different grain sizes (50, 100, 250, 500 and 1000 μm).

Figure 6 shows a scatter plot of the modeled MISR narrowband versus the modeled broadband albedo for all the cases mentioned above. The scatter to the right of the curves is a result of the dependence of the narrow-broadband relationship with solar zenith angle. The scatter is most pronounced for the visible channels because the solar zenith effect on the albedo is greater in the near infrared than in the visible and thus, the visible channels do not show the same dependence on the solar zenith angle as does the broadband albedo. The offset of curves in figure 7 is a result of the different atmospheric profiles.

The dependence of the narrow-broadband relationship on solar zenith angle is enhanced for larger grain sizes and the effect is most pronounced at the shorter wavelengths. Limiting the solar zenith angles to less than or equal to 70° results in a more linear relationship at shorter wavelengths. To a lesser extent, grain size differences cause some non-linearity in the relationship between the narrowband and broadband albedo.

The modeling results suggest that a non-linear relationship would be more applicable for the conversion from a narrowband to a broadband albedo. Furthermore, the model results also suggest that different relationships are needed for different atmospheric profiles.

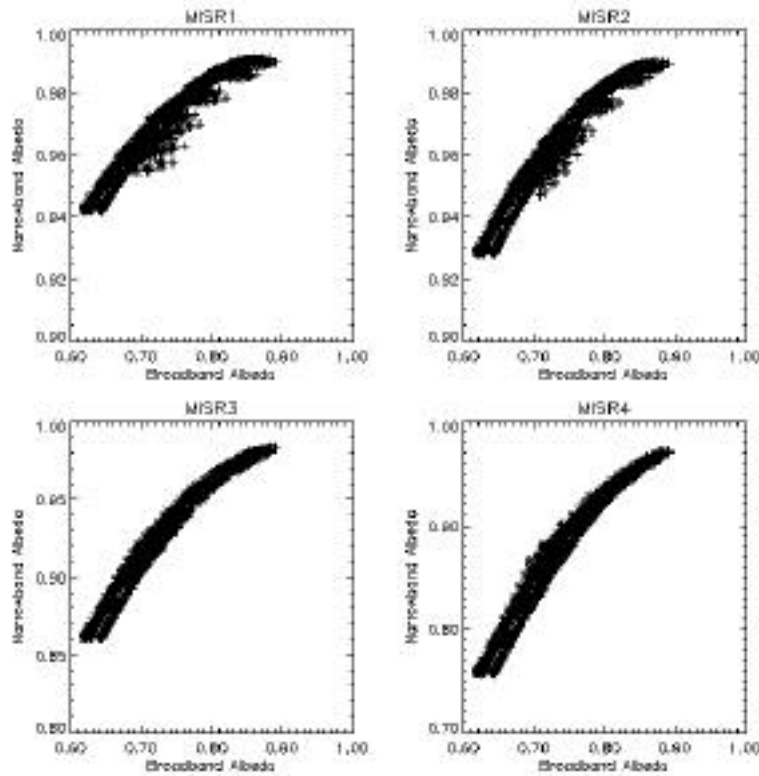


Figure 6. Modeled narrowband to broadband relationships for the MISR channels. Data include all grain sizes, all optical depths, all aerosol types and both arctic summer and arctic winter atmospheric profiles.

2.3 Comparison of MODIS and MISR albedos with in situ data

We are using a set of 15 automated weather stations (AWSs) on the Greenland ice sheet for broadband albedo validation measurements. As part of their instrumentation suite, each AWS has an upward and downward looking Licor pyranometer. Calibrations are applied to convert the Licor measurements to a broadband albedo, representing the spectral range from $0.35 - 3.0 \mu\text{m}$. AWS data are automatically transmitted to the University of Colorado and are made available to this project through the efforts of Dr. Konrad Steffen and Dr. Jason Box, both at CU. The data are first used to identify clear sky dates and times that coincide with MODIS and MISR data. We use the MODIS and MISR L1B2 data (calibrated radiances at the top-of-atmosphere). Locally-developed software is then used to read in the files and produce top-of-atmosphere BRF values. Solar and viewing geometry data as well as geographic coordinates are processed into additional files. The image data are then atmospherically-corrected using our version of 6S to obtain surface HDRFs. A lookup table program is then run that pulls out the appropriate conversion factors based on solar and viewing geometries and the proportions of direct and diffuse irradiance at the surface. Two different regression models were used for MODIS: one that uses channels 1-2 and another that uses channels 3-5. As described in the year 1999-2000 progress report, statistical tests indicate that using additional channels does not improve the regression. Furthermore, examination of MODIS radiance data indicates that channels 8-19 and 26 are saturated over snow.

Results for two sites, the ETH/CU camp (69.5°N, 49.5°W, elev. 1150 m) and the Summit station (72.5° N, 38.5°W, elev. 3220m) are presented here. Five MODIS images were acquired for the period May 24 – June 2, 2000 (because of its narrow orbital swath, no concurrent MISR data were available).

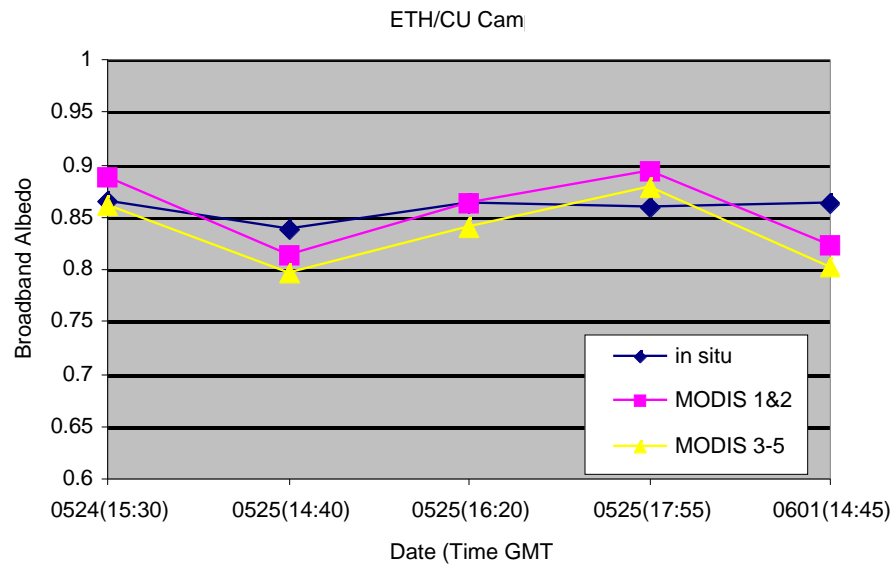


Figure 7. MODIS broadband albedo estimates compared with broadband measurements at the ETH/CU camp, on the western edge of the Greenland ice sheet.

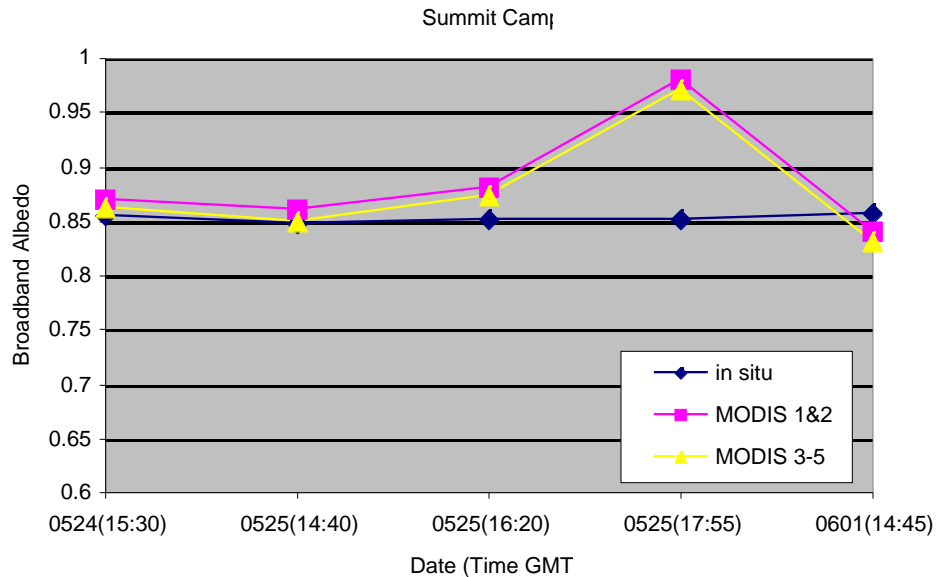


Figure 8. MODIS broadband albedo estimates compared with broadband measurements at the Greenland Summit station, at the central highpoint of the ice sheet. Data for May 25 (17:55 GMT) show how, for large viewing zeniths, the broadband albedo estimate is sensitive atmospheric characterization.

Atmospheric measurements made by Dr. Stroeve on May 25 at the ETH/CU camp were used as input to 6S for atmospheric correction of the imagery. Figure 7 compares MODIS broadband albedo estimates with the ground-based broadband albedo measurements at the ETH/CU camp. The overall results are in good agreement with absolute albedo differences less than 0.05, except for June 1 when the MODIS 3-5 regression model produced an albedo that was .07 below that of the measured value. These differences appear to reflect the sensitivity of the broadband estimates to atmospheric characterization. This is further demonstrated in figure 8, which shows the broadband estimates over the Summit station. The image collected at 17:55 GMT on May 25 had a viewing zenith of 57.7° , while the viewing zeniths for the other images ranged from 12.9° to 37.7° . The atmospheric correction was based on measurements taken at an elevation over 2000m lower than the Summit station. As long as the viewing zenith is relatively small, the atmospheric influence on the albedo estimate is relatively small. A future task is to re-run the atmospheric correction for these images (and others) using different atmospheric profiles, different aerosol types, and a range of optical depths to compute error bars for the albedo estimates.

An example of MISR broadband albedo retrievals is shown for an image over the ETH/CU camp acquired on August 12, 2000. At the time of the overpass, melt ponds dotted the surface. Data were extracted from the pixels corresponding to the ETH/CU camp. Only the 275m data were used in this analysis so that melt pond pixels could be excluded. Thus, only the red channels are available at all viewing angles; the nadir camera has all four MISR channels. Currently, the regression model uses only the multispectral data from the nadir camera, though it may be advantageous to incorporate data from additional cameras in future regression model improvements.

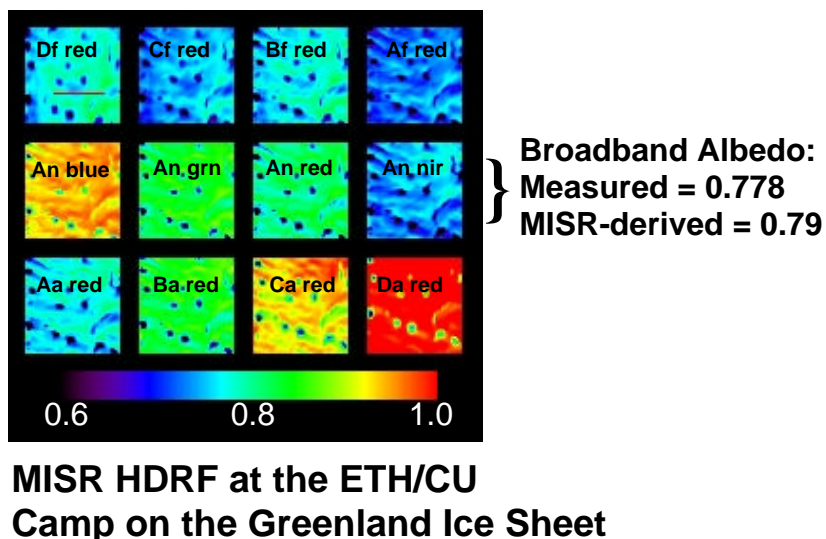


Figure 9. MISR multispectral nadir values were used to convert HDRF values to spectral albedo and from spectral albedo to narrowband albedo. Each subset is 13.75km x 13.75km. The MISR broadband albedo estimate is in excellent agreement with the measured value for this date.

In summary, these results indicate that the overall methodology of converting top-of-atmosphere multispectral BRF values to surface broadband albedo is sound, resulting in errors that are in the expected range. Future efforts are required to more definitively quantify the error bounds on albedo estimates, particularly with regard to atmospheric characterization.

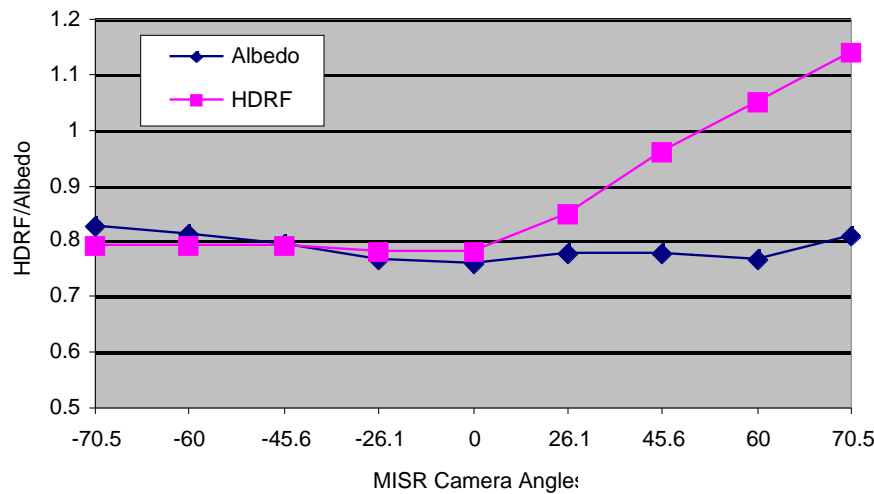


Figure 10. MISR HDRF and narrowband albedo values in the MISR red channels only. Though the surface HDRF values vary from 1.15 to .79, the albedo values (computed using the DISORT-derived conversion factors) only vary by 0.04.

3. Collaborations

We continue to work closely with members of both the MISR and MODIS Science Teams. On the MODIS side, we are working with Dr. Dorothy Hall and Dr. Andrew Klein to coordinate validation priorities and activities. We co-authored an article in which we describe the development of the prototype MODIS snow albedo algorithm.

Collaborations with the MISR team have also been very successful. The MISR validation group supported our efforts in Colorado this February-March, providing instrumentation and technical support for our ground experiment.

In related work, we are involved in an EO-1 investigation entitled “Advancing Glaciological Applications of Remote Sensing with EO-1” (Robert Bindshadler, PI). We are calculating broadband albedo from the Hyperion instrument on the EO-1 satellite using direct integration over the numerous spectral channels and comparing these estimates to our regression-based broadband estimates from MODIS and MISR. We share many validation sites between the two projects and anticipate that the comparisons will yield useful information about the different sensors and approaches to computing albedo, particularly with regard to spectral vs. multiangle approaches.

4. Planned Work for 2001-2002

The main objective of the work for the year 2001-2002 is to compile all error estimates for the MODIS and MISR narrowband and broadband albedo retrievals into a complete error budget. This will entail the following tasks:

1. Complete processing and analysis of MODIS and MISR data for a full summer season at AWS sites on the Greenland ice sheet (we estimate 30 MODIS and 10 MISR clear sky images) and compare with in situ albedo measurements

2. Compute broadband albedos for all images, using the full range of atmospheric characterizations (different atmospheric profiles, aerosol types, and optical depths) to give error bounds on the albedo estimate
3. Determine changes in error bounds for changes in target elevation, viewing zenith, and solar zenith
4. Complete analysis of MODIS and MAS data for the Colorado field experiment and compare with AirMISR, ASD, albedometer, and PARABOLA data for final snow BRDF validation
5. Release all processed data and lookup table values via the project website
6. Submit journal publication on validation of snow BRDF model.

Timeline:

Oct – Nov 2001	Complete processing of MODIS and MISR data for Greenland (Task 1)
Dec - Jan 2002	Compute broadband albedos for Greenland data using all atmospheric characterizations; test for effects of elevation, solar zenith and viewing zenith (Tasks 2-3)
Feb - Mar 2002	Complete MODIS and MAS data analysis for Colorado experiment (Task 4)
Apr - May 2002	Write up journal publication and release all data to the public (Tasks 5-6)

Relevant Publications for 2000-2001

Nolin, A. W., T. Scambos, J. C. Stroeve, and F. Fetterer, Cryospheric applications of MISR data. *Submitted to IEEE TGARS special issue on MISR.*

Stroeve, J. C. and A. W. Nolin, Comparison of narrowband-to-broadband conversions for MISR, MODIS, and AVHRR. *Submitted to IEEE TGARS special issue on MISR.*

Nolin, A. W. and S. Liang, Progress in bidirectional reflectance modeling and applications for surface particulate media: Snow and soils, *Remote Sensing Reviews*, 18, 307-342, 2000.

Liang, S., J. C. Stroeve, I. F. Grant, A. H. Strahler, and J. P. Duvel, Angular corrections to satellite data for estimating Earth radiation budget, *Remote Sensing Reviews*, 18, 103-136, 2000.

Nolin, A. W. and A. Frei, Remote Sensing of Snow and Snow Albedo Characterization for Climate Simulations, chapter in: "Remote Sensing and Climate Simulations: Synergies and Limitations", Edited by Martin Beniston, *Advances in Global Change Research*, Kluwer, The Netherlands, 159-180, 2001.